Journal of CO2 Utilization 98 (2025) 103154

Contents lists available at ScienceDirect

Journal of CO2 Utilization

journal homepage: www.elsevier.com/locate/jcou

CO_2 conversion into formic acid with CO-containing hydrogen gas over a heterogenized Ru catalyst

Hongjin Park, Seokyeong Moon, Sungho Yoon *

Department of Chemistry, Chung-Ang University, 84 Heukseok-ro, Dongjak-gu, Seoul 06974, Republic of Korea

ARTICLE INFO

Keywords:
CO_2 hydrogenation into formate
CO poisoning effect on Ru-MACHO-POMP
Metal leaching durability
Sustainable catalytic activity
Reversible active structure

ABSTRACT

To achieve cost-competitive CO_2 hydrogenation processes, it is desirable to utilize gray hydrogen, which typically contains 1–3 mol% CO. However, previously reported catalysts have been severely affected by CO poisoning, leading to metal aggregation, active site leaching, and structural deactivation. The CO tolerance test of Ru-MACHO-POMP (porous organometallic polymer) confirmed that the catalyst maintained activity during CO_2 hydrogenation to formic acid even under high CO concentrations (12.5 mol%). Through various characterization methods analyzing catalytic active sites, it was found that the catalytic activity was reversibly restored due to reversible binding of CO to Ru active sites, enabling the regeneration of the original active structure. These findings highlight Ru-MACHO-POMP as a sustainable and economically viable catalyst for industrial CO_2 hydrogenation processes.

1. Introduction

Carbon dioxide (CO_2), emitted from human industrial activities, has been widely recognized as a primary driver of climate change [1–5]. To address the continuous rise in CO_2 emissions, sustainable mitigation strategies such as Carbon Capture and Utilization (CCU) technologies have been developed to capture and convert emitted CO_2 into valuable resources [2,6–13]. CO_2-derived value-added products include cyclic carbonates and polycarbonates produced via reactions with epoxy compounds, as well as formic acid, formaldehyde, and methanol generated through hydrogenation [14]. Among these, production of formic acid (FA) from CO_2 is considered one of the most efficient CO_2 reduction pathways due to its 100 % atom economy and 95.7 wt% CO_2 contribution (Eq. (1)) [12,15–18].

$$CO_2 + H_2 \rightleftharpoons HCO_2H \quad (1)$$

The current state of research on FA production has progressed through optimization of catalytic activity and reaction efficiency, leading to the development of process systems demonstrating high productivity and stability [19–21]. Various heterogeneous catalysts have been applied in continuous flow reactors, with pilot-scale feasibility being actively tested [17,21–28]. For cost-competitive processes, the use of gray hydrogen is essential, as it provides sufficient economic feasibility [21,29–33]. Gray hydrogen is produced through steam methane reforming (SMR, Eq. (2)) and undergoes a water-gas shift reaction (WGSR, Eq. (3)), resulting in a product that typically contains 1–3 mol% CO [34–37].

$$CH_4 + H_2O \rightleftharpoons CO + 3H_2 \quad (2)$$

$$CO + H_2O \rightleftharpoons CO_2 + H_2 \quad (3)$$

Conventional heterogeneous catalysts used in CO_2 hydrogenation have been shown to suffer from CO poisoning, leading to severe issues in catalytic sustainability such as metal aggregation, active metal leaching, and deactivation of active site [38–70]. Furthermore, it has been reported that CO is generated as a byproduct during CO_2 hydrogenation with these catalysts [21,22,39,46,49,69–73]. In practical applications, unreacted H_2 and CO_2 are typically recycled, which could result in the accumulation of CO, potentially exacerbating its detrimental effects on the catalyst. Therefore, even if pure hydrogen becomes economically viable for industrial use in the future, the issue of CO generated during the reaction itself remains unavoidable [21,29–37]. This underscores the necessity for catalysts with intrinsic tolerance to CO.

Interestingly, the Ru-MACHO catalyst (Fig. 1, a), which is widely recognized as an excellent hydrogenation catalyst, has been reported to undergo structural changes due to the reaction byproduct CO, yet it is proposed to be reversible in the presence of hydrogen [54]. This characteristic offers a significant advantage, as it suggests that

* Corresponding author.
E-mail address: sunghoyoon@cau.ac.kr (S. Yoon).

https://doi.org/10.1016/j.jcou.2025.103154
Received 1 April 2025; Received in revised form 30 May 2025; Accepted 12 June 2025
Available online 17 June 2025

hydrogenation can still proceed even when utilizing CO-containing flue gas or gray hydrogen. Recently, our group successfully synthesized Ru-MACHO-POMP (porous organometallic polymer) through an optimized heterogenization method for the Ru-MACHO catalyst [28]. This catalyst exhibited a productivity of 36,100 $kg_{FA.}/(kg_{cat.}\cdot day)$ in CO_2 hydrogenation into formate, highlighting its potential for industrial-scale applications (Fig. 1, a). However, despite its remarkable catalytic activity, there have been no reports on its performance in reactions involving CO-containing environments.

In this study, the CO tolerance of the Ru-MACHO-POMP catalyst was investigated to evaluate its potential for industrial applications (Fig. 1, b). The results demonstrated that formate production via CO_2 hydrogenation was feasible even under excess CO conditions (12.5 mol%). Structural changes involving the di-CO configuration were analyzed using Fourier-transform infrared spectroscopy (FT-IR) and X-ray photoelectron spectroscopy (XPS). Additionally, recycling tests conducted under CO-free conditions confirmed the catalyst's reversible recovery to its pristine active structure.

2. Experimental section

2.1. Materials

All reagents utilized in this study were obtained from commercial sources and used as provided, without additional purification. Ru-MACHO, anhydrous dichloromethane, and triethylamine (99.5 %) were sourced from Sigma-Aldrich, while anhydrous aluminum chloride (99.999 %) was purchased from Alfa Aesar. Dichloromethane, hydrochloric acid, and ethanol for washing purposes were supplied by Daejung Chemicals. The gases H_2, CO_2, and CO were utilized with a purity of 99.999 %. All distilled water used during the experiments was prepared through single distillation. The synthesis of Ru-MACHO-POMP (**1**) was conducted following previously published methods [28].

2.2. Analysis

Ru-MACHO-POMP (**1**) was dried overnight at 60 °C in a vacuum oven prior to characterization measurements. Surface morphology and metal dispersion of the catalyst were analyzed using a Carl Zeiss SIGMA-300 field emission scanning electron microscope (FE-SEM) and energy-dispersive spectrometer (EDS) operating at an accelerating voltage of 17.0 kV. The Ru content in the catalyst (wt%) was determined through inductively coupled plasma optical emission spectrometry (ICP-OES) using an Agilent 720 system at the KAIST Analysis Center for Research Advancement (KARA). Catalyst samples were pretreated with a microwave-assisted acid digestion system before analysis. X-ray powder diffraction (PXRD) patterns were recorded using a Rigaku MiniFlex 600 diffractometer equipped with a Cu Kα radiation source (λ = 1.5418 Å), operated at 30 kV and 15 mA with a maximum output power of 600 W. A D/teX Ultra silicon strip detector was used for high-resolution data acquisition. Measurements were performed in reflection mode over a 2θ range of 30° to 90°, with a scan speed of 1°/min and a step size of 0.01°.

Fourier-transform infrared spectroscopy (FT-IR) was conducted on a Nicolet iS 10 equipped with a mercury-cadmium-telluride (MCT) detector and a diamond crystal attenuated total reflectance (ATR) accessory (Thermo Fisher Scientific). To evaluate the Ru oxidation state at the catalyst's active sites, X-ray photoelectron spectroscopy (XPS) measurements were carried out using an Al Kα excitation source ($h\nu$ = 1486.6 eV) under ~3×10^{-9} mbar with a concentric hemispherical analyzer (K-alpha+, Thermo Fisher Scientific). The binding energy of C 1 s at 284.6 eV was used for calibration.

The formic acid produced during catalytic activity was quantified using a Waters Arc high-performance liquid chromatography (HPLC) system with a refractive index detector (RID) and an Aminex HPX-87H column. The column temperature was maintained at 50 °C, with a 5.00 mM H_2SO_4 mobile phase flowing at 0.6 mL/min. FA quantification was performed using a calibration curve ranging from 0.0125 to 5.00 M,

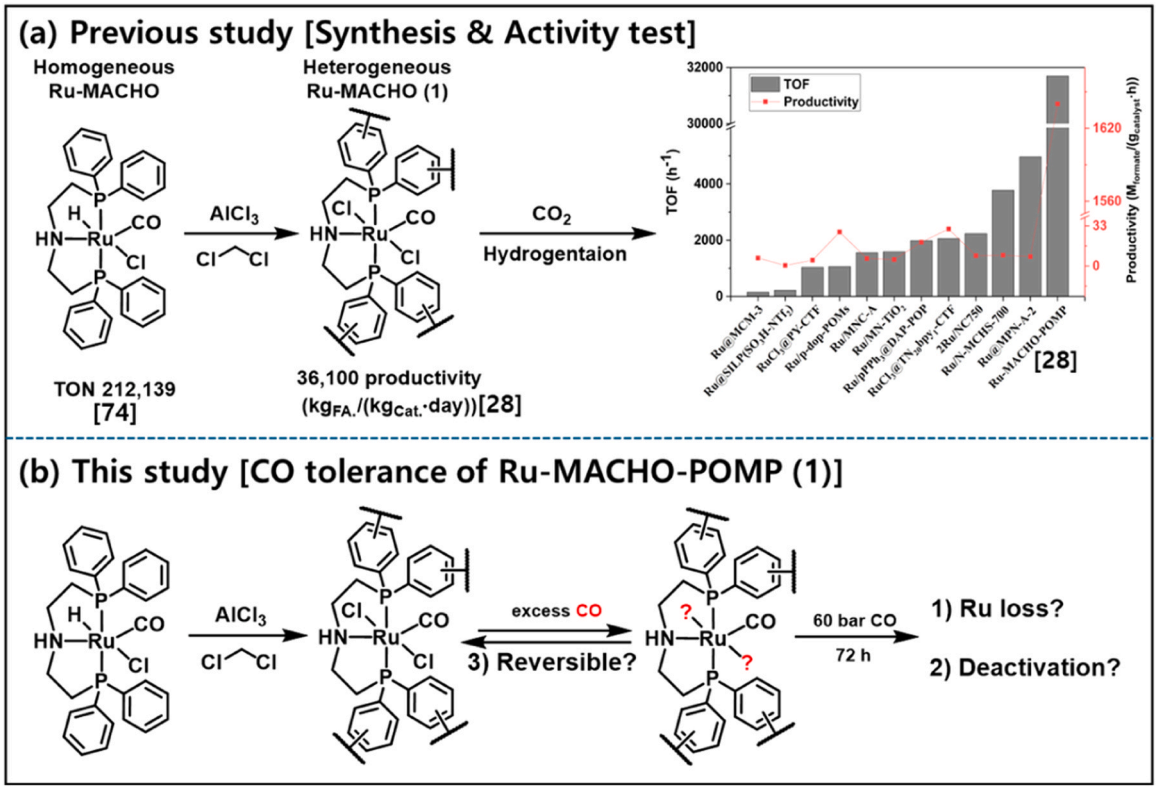

Fig. 1. The synthesis of Ru-MACHO-POMP (**1**), its potential for CO_2 hydrogenation activity, and three potential issues that may arise during CO tolerance experiments in hydrogenation catalysis [28].

constructed with seven data points and a correlation coefficient (R^2) of 0.999999. ^{1}H Nuclear Magnetic Resonance (NMR) spectra were recorded on a Varian 600 MHz NMR spectrometer using D_2O as the solvent [δ = 4.79 ppm (^{1}H NMR, s)]. Gas chromatography (GC) analyses were performed using a YL-6500 system (Younglin, Korea) equipped with flame ionization and thermal conductivity detectors. Nitrogen was used as the carrier gas at a flow rate of 10 mL/min, and the detection limit for gaseous components was greater than 1 ppm (> 0.0001 %).

2.3. General procedure for CO_2 hydrogenation into formate, CO deactivation, and recycling tests

Primarily, a custom-made 50 mL tube reactor and an oil bath were utilized for the hydrogenation reactions. The reactor was charged with the catalyst (Ru-MACHO-POMP, **1**), deionized water (5.8 mL), and triethylamine (3.0 g, 4.2 mL). The CO partial pressure and CO_2 pressure, as defined by the experimental setup, were introduced into the reactor. After allowing 20 min for CO_2 saturation in the solvent, CO_2 was repressurized up to set pressure. Subsequently, the remaining pressure was filled with H_2. Once the desired reaction temperature was reached, the reaction was carried out at 600 RPM for the specified duration.

Upon completion of the reaction, the reactor was removed from the oil bath and allowed to cool to room temperature before the pressure was released. The reactor was then opened, and a sample was collected for quantitative analysis of the generated formic acid using HPLC. For reuse experiments, the catalyst was filtered using a syringe filter. For subsequent reaction cycles, the filtered catalyst was reintroduced into the reactor with 3 M TEA as the reaction solvent.

3. Results and discussion

3.1. Ru-MACHO-POMP catalyst and necessity for CO tolerance evaluation

The Ru-MACHO catalyst, a PNP-based catalyst, has demonstrated exceptional catalytic performance in CO_2 hydrogenation into formate, achieving a maximum TON of 212,139 with an 85 % yield [74]. It is recognized as one of the most effective homogeneous catalysts studied for this reaction [75]. To leverage the advantages of this homogeneous catalyst in a heterogeneous form, multiple attempts were made, ultimately leading to the successful synthesis of a stable Ru-MACHO-POMP (**1**) catalyst using a solvothermal method [28]. This catalyst incorporates 10 wt% of highly active Ru sites, achieving a productivity of 36,100 $kg_{FA.}/(kg_{cat.}\cdot day)$, which is approximately 50 times higher than the maximum productivity reported for previously studied Ru catalysts (Fig. 1, a). However, catalysts with practical potential must undergo rigorous CO tolerance evaluations to ensure their feasibility for industrial applications. The detailed synthetic procedures and structural characterization of the Ru-MACHO-POMP catalyst, including its coordination structure, porosity, and metal incorporation method, were thoroughly described in a previous study [28]. The present study focuses on evaluating CO tolerance and the reversibility of structural changes under CO-containing conditions, which are critical properties for practical catalyst applications.

3.2. Impact of CO on catalyst activity and stability

When forming FA via the hydrogenation of CO_2, the reaction becomes thermodynamically favorable in the presence of a base [76,77].

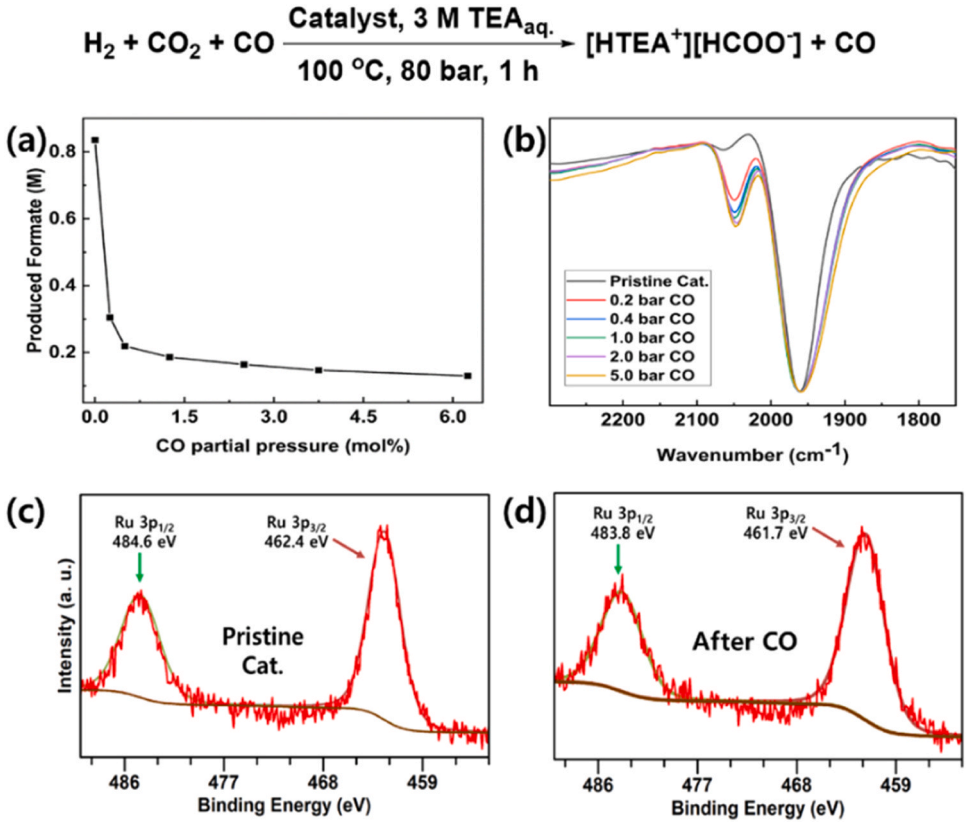

Fig. 2. (a) CO_2 hydrogenation activity graph of Ru-MACHO-POMP (**1**) by CO partial pressure (mol%) [a], (b) FT-IR results of **1** used in CO poisoning experiments, (c) deconvoluted peaks of Ru3*p* binding energy for pristine **1**, and (d) deconvoluted peaks of Ru3*p* binding energy for 1 used in CO-containing CO_2 hydrogenation experiments. [a] Reaction conditions: Ru-MACHO-POMP (5 mg), 3 M TEA (10 mL), total pressure of 80 bar (CO partial pressure + remaining pressure with H_2:CO_2 = 1:1) in a 50 mL tube reactor, T = 100 °C, time = 1 h.

Thus, triethylamine (TEA), commonly used in reported hydrogenation catalysts, was employed as the base. The experiments were conducted in a 50 mL tube reactor at 100 °C for 1 h using 3 M TEA (10 mL) & 5 mg of catalyst **1** (Fig. 2, a). The produced formate was quantified using HPLC analysis and calculated based on a pre-established calibration curve. To confirm the formation of other possible products from CO_2 hydrogenation, including methanol, CO, and CH_4, additional analyses using NMR and GC were conducted (Fig. S1). The results showed that methanol was not detected, and no formation of CO or CH_4 was observed. These results indicate that formate was the predominant product formed during CO_2 hydrogenation over Ru-MACHO-POMP under the tested reaction conditions. Therefore, all subsequent experiments were carried out under the same conditions. Under CO-free background conditions, a formate concentration of 0.835 M was produced. To investigate the effect of CO on the activity of catalyst **1**, the total pressure was fixed at 80 bar (H_2:CO_2 = 1:1), with the mol% of CO in the total pressure varied between 0.25 and 6.25 mol% (Fig. 2, a). As a result, with an increase in CO partial pressure from 0.25 mol% to 0.5 mol%, the catalytic activity decreased from 36.4 % to 26.2 %. However, beyond this point, further increases in CO concentration did not significantly affect catalytic activity, which remained stable. This indicates that while CO strongly influences the initial rate of activity reduction, it has minimal additional impact once a threshold concentration of 0.5 mol% is exceeded.

To verify whether the activity loss of catalyst **1** was caused by metal leaching due to CO poisoning, the residual Ru content of the catalyst before and after use was measured using ICP-OES (Table. S1). Both the fresh and used catalysts remained at 10 wt% Ru, confirming that no metal leaching occurred due to CO exposure. To further confirm CO tolerance, long-term poisoning experiments were conducted under harsher conditions with only 60 bar CO and 3 M TEA as a basic solvent for 72 h at 120 °C. The catalyst was then separated, and their metal content was analyzed using ICP-OES, while catalyst **1** retained its initial 10 wt% Ru content even after the experiment (Table S1). This demonstrates that the Ru-MACHO PNP-based catalyst **1** exhibits excellent resistance to metal leaching under CO conditions, as no Ru leaching was observed. To further assess the possibility of Ru aggregation within the porous framework—which could result in long-term deactivation even without leaching—powder X-ray diffraction (PXRD) analysis was conducted on the catalyst recovered after exposure to 60 bar CO. No detectable Ru-related peaks were observed (Fig. S2), confirming that aggregation of Ru particles did not occur under these conditions.

In general, the CO-induced activity decline in catalysts used for hydrogenation can be categorized into three main reasons. The first issue is the leaching of active metals caused by CO. The second is the structural modification of the active site by CO, leading to a gradual decrease in activity and eventually resulting in an inactive structure. The third issue is the irreversible transformation of the inactive structure, preventing the catalyst from reverting to its original active form and rendering it unusable (Fig. 1).

When metal leaching at the active site is ruled out, one possible cause of activity loss in heterogeneous catalysts is morphological changes, such as pore blockage or the collapse of the heterogeneous framework, which alter the catalyst's porosity [28]. A decrease in porosity reduces the probability of substrates reaching the central active metal sites, potentially lowering catalytic efficiency [78–83]. To investigate this issue, the porosity of the recovered catalyst after the reaction was analyzed using N_2 isotherm measurements and calculated via the BET method (Fig. S3). The post-reaction Ru-MACHO-POMP retained its external morphology and exhibited a stable N_2 isotherm graph, demonstrating its durability. These results confirm that morphology-related changes, commonly observed in heterogeneous catalysts, do not occur in this system.

Since the Ru active atmosphere of catalyst **1** was confirmed to remain stable even under harsh conditions with excess CO (60 bar), the observed activity decrease with increasing CO partial pressure suggests structural changes in the active site. According to previous reports, Ru-MACHO undergoes transformation into a di-CO structure in the presence of CO, leading to a significant reduction in catalytic activity [54]. As catalyst **1** employs Ru-MACHO as its active site, similar behavior is anticipated (Fig. 1). To investigate structural changes in the active site under varying CO partial pressures, the catalysts were recovered via simple filtration and analyzed using FT-IR and XPS (Fig. 2, b-d). Both the pristine **1** catalyst and the catalysts used under 0.25 mol% and 6.25 mol % CO conditions showed the characteristic vibration mode peak of the mono-CO ligand (1960 cm^{-1}, Ru-CO) associated with Ru-MACHO (Fig. 2, b). Additionally, the initial **1** catalyst exhibited significant reduction of the Ru-H vibration mode peak (2065 cm^{-1}), which is known to disappear due to the Friedel-Crafts reaction. For catalysts used under 0.25–6.25 mol% CO conditions, the intensity of the di-CO peak (2050 cm^{-1}) increased with rising CO concentrations [54]. Notably, a sharp increase in the di-CO vibration mode peak was observed up to 0.4 bar CO (0.5 mol%), suggesting that the transformation to the di-CO structure is a primary cause of the significant activity reduction at this pressure [54]. Beyond this point, the continued increase in the di-CO peak intensity indicates an accumulation of the di-CO structure within the recovered catalyst. To confirm the Ru environment changes observed via XPS analysis was conducted to examine the Ru binding energy (Fig. 2, c, d). The Ru3*p* deconvoluted peaks (Ru3$p_{5/2}$ and Ru3$p_{3/2}$) of the catalyst used under 6.25 mol% CO conditions exhibited a decreasing trend in binding energy compared to pristine 1. This indicates that Ru-Cl in the initial catalyst was replaced with Ru-diCO under CO conditions, resulting in an increase in the electron density of Ru. These findings are consistent with the trends observed in the FT-IR analysis. This indicates that the reduction in catalytic efficiency caused by CO can be attributed to additional CO binding. The observed phenomenon is consistent with the behavior of homogeneous Ru-MACHO catalysts, as the POMP catalyst shares the same fundamental active structure [54].

Through the characterization of the catalysts used in CO partial pressure experiments, it was confirmed that the active Ru-diCO structure was preferentially formed even at low CO concentrations (0.25 mol %), leading to changes in catalytic activity. Furthermore, additional formation of diCO active structures was observed in catalysts recovered from CO conditions exceeding 0.5 mol% (Fig. 2, b). These findings suggest that catalyst **1** rapidly transition to the diCO structure upon initial CO exposure. However, further investigation is required to determine whether all Ru active sites are fully substituted by CO, ultimately causing catalyst deactivation. To address this, continuous CO_2 hydrogenation experiments were conducted under excess CO conditions (10 bar, 12.5 mol%) using the **1** catalyst (Fig. 3). Catalyst **1** maintained activity for 16 h under excess CO and ultimately produced 2.477 M of

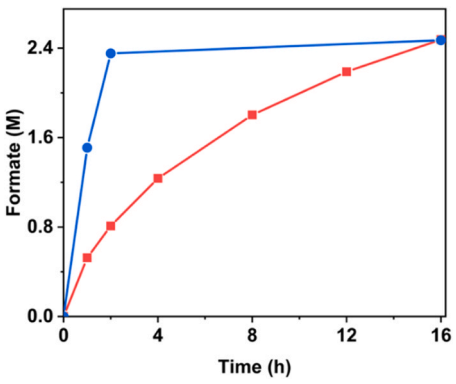

Fig. 3. Graph of formate activity for CO_2 hydrogenation using Ru-MACHO-POMP under excess CO conditions [a]. [a] Reaction condition: Ru-MACHO-POMP (20 mg), 3 M TEA (10 mL) in tube reactor (50 mL), T = 100 °C, red line: 12.5 mol% of CO (10 bar) + 70 bar (H_2:CO_2=1:1), blue line: CO-free + 70 bar (H_2:CO_2=1:1) in 50 mL tube reactor.

formate (Fig. 3, red line). This result is comparable to the 2.471 M formate generated under CO-free conditions over 16 h, indicating that the catalyst sustained activity up to the product saturation point (Fig. 3, blue line). These findings demonstrate that catalyst **1** can maintain consistent activity and achieve the product saturation point even in the presence of excess CO. Thus, catalyst **1** is suggested to be capable of maintaining a certain level of activity under high CO conditions.

3.3. Reversible recovery and catalyst recycling

Catalyst **1** exhibited a decrease in efficiency due to the transformation of its active structure into a di-CO configuration even under low CO concentrations (Fig. 2). However, it maintained activity for extended periods and produced up to the product saturation point under excess CO conditions (Fig. 3). This suggests that while the catalyst rapidly transitions to a di-CO structure, it does not transform into the fully inactive tri-CO structure or, if such a transformation occurs, it can be reversibly recovered in the presence of H_2. To test this hypothesis, the catalyst used under 12.5 mol% CO (10 bar) was recovered and reused under CO-free conditions to evaluate its recovery in both activity and structure (Fig. 4, a). Under 70 bar CO-free conditions, the catalyst exhibited an activity of 0.617 M. When the reaction was conducted at 80 bar with excess CO, the activity decreased to approximately 20 % (0.139 M, Fig. 4, a, entry 2) of that under CO-free conditions. However, when the catalyst used in excess CO was separated using a syringe filter and reused under CO-free hydrogenation conditions, its activity partially recovered to 0.486 M (~80 %, Fig. 4, a, entry 3), and a second reuse experiment showed complete recovery to the initial activity level observed under CO-free conditions (Fig. 4, a, entry 4). To confirm whether the structure of the reused catalyst was restored, FT-IR and XPS analyses were conducted (Fig. 4, b-d). For comparison, the initial catalyst subjected to CO-free conditions was also analyzed. The catalyst under CO-free conditions showed that Ru-Cl was replaced with Ru-H through the action of H_2, as evidenced by the reappearance of the Ru-H vibration mode peak (2065 cm^{-1}) in the FT-IR results (Fig. 4, b). Furthermore, XPS revealed a decrease in the binding energy of $Ru3p_{1/2}$ and $Ru3p_{3/2}$ compared to the initial **1** catalyst (Fig. 4, c), indicating an increase in electron density due to the replacement of Ru-Cl with Ru-H (Figs. S4, S5) [28,82,84]. Remarkably, the reused catalyst displayed FT-IR and XPS results identical to those of the catalyst used once under CO-free conditions (Fig. 4, b, d). This indicates that the catalyst was fully restored after the first reuse experiment and that the di-CO structure can reversibly recover to the original active configuration. Additionally, the second reuse experiment confirmed that the CO-modified catalyst fully recovered after a single CO-free hydrogenation cycle. This suggests that the Ru-CO or Ru-diCO catalytic cycle is predominantly determined by the relative concentrations of H_2 and CO in the reaction conditions. Therefore, catalyst **1** demonstrates resilience against complete deactivation in industrial conditions with low CO concentrations and exhibits potential for sustained application due to its recoverability.

3.4. Proposed catalytic mechanism under CO exposure conditions

Based on the results obtained thus far and the references cited, a mechanism is proposed for the active structures and expected catalytic cycle of catalyst **1** during the hydrogenation process in the presence of CO (Fig. 5). The structures mentioned in the proposed mechanism are categorized as (a) to (i) and are referred to as (a) form to (h) form for simplicity. The active structure of catalyst **1**, Ru-MACHO, is activated from (a) form to (b) form during the hydrogenation process by the added base, triethylamine (denoted as R_3N) [28]. As a hydrogenation catalyst, Ru-MACHO can undergo H_2 cleavage, forming the reported (c) form through interaction with H_2 [28,74,85–88]. Subsequently, HCl is removed by R_3N, forming the active (d) form. Following the reported mechanisms of Ru-MACHO and other Ru hydrogenation catalysts, H_2 cleavage generates Ru-H (e), which undergoes CO_2 insertion (f) to form formate. Under typical conditions, Ru-MACHO transitions to the reported resting state, (g) form, at the end of the reaction (Fig. 4, b;

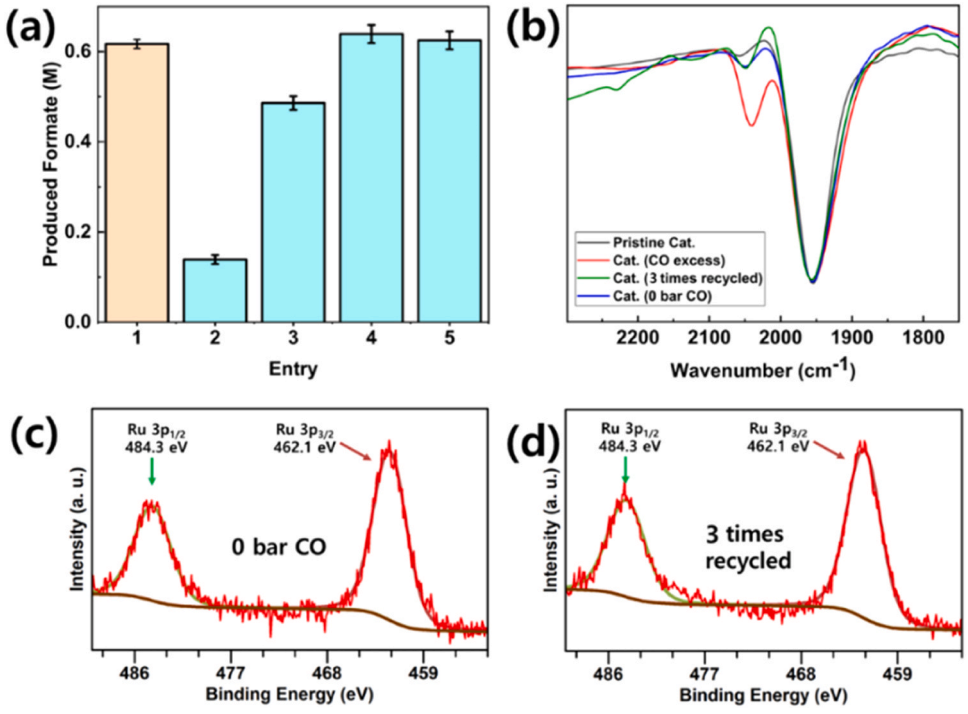

Fig. 4. a) Recovery and recycling experiments of Ru-MACHO-POMP (**1**) after CO poisoning (entry 2 [a], entry 1 & 3–5 [b]), (b) FT-IR graphs of catalysts obtained after CO poisoning experiments, (c) Deconvoluted Ru3*p* binding energy peaks of **1** after experiments conducted under CO-free conditions, and (d) Deconvoluted Ru3*p* binding energy peaks of **1** after recovery and recycling experiments following CO poisoning. Reaction condition: Ru-MACHO-POMP (10 mg), 3 M TEA (10 mL) in tube reactor (50 mL), $T = 100$ °C, time = 0.5 h, [a] CO-free + 70 bar (H_2:CO_2=1:1), [b] with CO (10 bar) + 70 bar (H_2:CO_2=1:1).

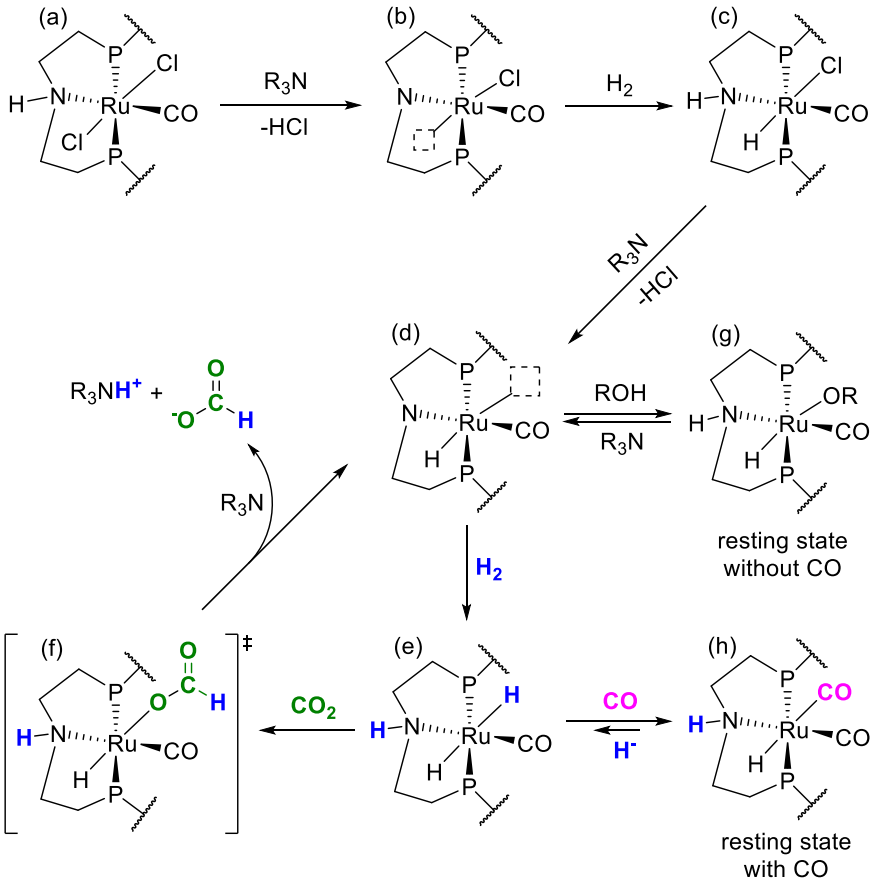

Fig. 5. Proposed mechanism of CO_2 hydrogenation and its behavior in the presence of CO using the Ru-MACHO-POMP catalyst.

Figs. S4, S5). Upon re-entry into the reaction, the base in the reaction medium can reactivate (g) form into the active (d) form [28,42,48,82,89,90].

In the presence of CO, the (e) state can transition to (h) form [54]. Furthermore, activity comparison graphs and FT-IR results under low CO partial pressure conditions indicate that the transition from (e) form to (h) form is dominant even at low CO concentrations (Fig. 2, a–b). Since (h) form is predominantly generated under CO conditions, it is proposed to be the resting state in the presence of CO (Fig. 2, b). Additionally, even under excess CO conditions, catalytic activity was not entirely lost (Fig. 3). The generated di-CO (h) form was completely restored to the pristine catalyst's activity level when reused under CO-free conditions (Fig. 4, a), confirming that (h) form can be reversibly recovered to (e) form via hydride formation (Fig. 4, b-d).

4. Conclusion

The recently developed Ru-MACHO-POMP (**1**) is a PNP-based organometallic catalyst that demonstrates exceptional CO tolerance by maintaining strong metal-ligand bonds even under excess CO conditions. Activity comparisons under varying CO partial pressures revealed an initial decrease in activity with increasing CO concentrations, followed by stabilization at a certain level. The activity loss was attributed to the rapid transition to a di-CO structure in the presence of CO, as confirmed through characterization of the used catalyst. Long-term experiments conducted under excess CO conditions showed that the catalyst did not undergo further deactivation. Despite structural changes induced by CO, the Ru-MACHO-POMP (**1**) catalyst retained its function as a sustainable catalyst, and the altered structure was shown to reversibly recover to its original active configuration through the competitive interaction of CO and H_2. This indicates that Ru-MACHO-POMP can maintain activity and easily recover its original structure despite structural changes caused by CO, effectively preventing metal leaching and deactivation observed in previous catalysts. This study provides a benchmark for CO tolerance that future catalysts for converting CO_2 to FA should achieve and serves as a critical foundation for developing catalysts applicable to economically competitive processes aimed at replacing conventional technologies, highlighting the need for further optimization of hydrogenation conditions such as temperature and pressure to enhance catalytic performance under CO-containing environments.

CRediT authorship contribution statement

Sungho Yoon: Writing – review & editing, Supervision, Project administration, Funding acquisition. **Seokyeong Moon:** Conceptualization. **Hongjin Park:** Writing – review & editing, Writing – original draft, Visualization, Validation, Supervision, Software, Resources, Project administration, Methodology, Investigation, Formal analysis, Data curation, Conceptualization.

Declaration of Competing Interest

The authors declare that they have no known competing financial interests or personal relationships that could have appeared to influence the work reported in this paper.

Acknowledgements

This work was supported by the DACU Project (RS-2023–00259920) and C1 Gas Refinery Value Up Technology Development Project (RS-2024-00466477) through the National Research Foundation of Korea

(NRF) funded by the Ministry of Science and ICT, and Future Planning, Republic of Korea. This research was supported by the Chung-Ang University Research Scholarship Grants in 2023.

Appendix A. Supporting information

Supplementary data associated with this article can be found in the online version at doi:10.1016/j.jcou.2025.103154.

Data availability

Data will be made available on request.

References

[1] A. Mikhaylov, N. Moiseev, K. Aleshin, T. Burkhardt, Global climate change and greenhouse effect, Entrep. Sustain. Issues 7 (4) (2020) 2897–2913, https://doi.org/10.9770/jesi.2020.7.4(21).
[2] K.O. Yoro, M.O. Daramola, CO2 emission sources, greenhouse gases, and the global warming effect, Adv. Carbon Capture (2020) 3–28, https://doi.org/10.1016/b978-0-12-819657-1.00001-3.
[3] A. Hartley, S. Turnock, What are the benefits of reducing global CO2 emissions to net-zero by 2050? Weather 77 (1) (2021) 27–28, https://doi.org/10.1002/wea.4111.
[4] M. Klöwer, M.R. Allen, D.S. Lee, S.R. Proud, L. Gallagher, A. Skowron, Quantifying aviation's contribution to global warming, Environ. Res. Lett. 16 (10) (2021), https://doi.org/10.1088/1748-9326/ac286e.
[5] P.M. Forster, C. Smith, T. Walsh, W.F. Lamb, R. Lamboll, B. Hall, M. Hauser, A. Ribes, D. Rosen, N.P. Gillett, M.D. Palmer, J. Rogelj, K. von Schuckmann, B. Trewin, M. Allen, R. Andrew, R.A. Betts, A. Borger, T. Boyer, J.A. Broersma, C. Buontempo, S. Burgess, C. Cagnazzo, L. Cheng, P. Friedlingstein, A. Gettelman, J. Gütschow, M. Ishii, S. Jenkins, X. Lan, C. Morice, J. Mühle, C. Kadow, J. Kennedy, R.E. Killick, P.B. Krummel, J.C. Minx, G. Myhre, V. Naik, G.P. Peters, A. Pirani, J. Pongratz, C.-F. Schleussner, S.I. Seneviratne, S. Szopa, P. Thorne, M.V. M. Kovilakam, E. Majamäki, J.-P. Jalkanen, M. van Marle, R.M. Hoesly, R. Rohde, D. Schumacher, G. van der Werf, R. Vose, K. Zickfeld, X. Zhang, V. Masson-Delmotte, P. Zhai, Indicators of Global Climate Change 2023: annual update of key indicators of the state of the climate system and human influence, Earth Syst. Sci. Data 16 (6) (2024) 2625–2658, https://doi.org/10.5194/essd-16-2625-2024.
[6] P. Gabrielli, M. Gazzani, M. Mazzotti, The Role of Carbon Capture and Utilization, Carbon Capture and Storage, and Biomass to Enable a Net-Zero-CO2 Emissions Chemical Industry, Ind. Eng. Chem. Res. 59 (15) (2020) 7033–7045, https://doi.org/10.1021/acs.iecr.9b06579.
[7] W. Gao, S. Liang, R. Wang, Q. Jiang, Y. Zhang, Q. Zheng, B. Xie, C.Y. Toe, X. Zhu, J. Wang, L. Huang, Y. Gao, Z. Wang, C. Jo, Q. Wang, L. Wang, Y. Liu, B. Louis, J. Scott, A.-C. Roger, R. Amal, H. He, S.-E. Park, Industrial carbon dioxide capture and utilization: state of the art and future challenges, Chem. Soc. Rev. 49 (23) (2020) 8584–8686, https://doi.org/10.1039/d0cs00025f.
[8] T.Td Cruz, J.A. Perrella Balestieri, J.M. de Toledo Silva, M.R.N. Vilanova, O. J. Oliveira, I. Ávila, Life cycle assessment of carbon capture and storage/utilization: From current state to future research directions and opportunities, Int. J. Greenh. Gas. Control 108 (2021), https://doi.org/10.1016/j.ijggc.2021.103309.
[9] M.A. Sabri, S. Al Jitan, D. Bahamon, L.F. Vega, G. Palmisano, Current and future perspectives on catalytic-based integrated carbon capture and utilization, Sci. Total Environ. 790 (2021), https://doi.org/10.1016/j.scitotenv.2021.148081.
[10] T.M. Gür, Carbon dioxide emissions, capture, storage and utilization: review of materials, processes and technologies, Prog. Energy Combust. Sci. 89 (2022), https://doi.org/10.1016/j.pecs.2021.100965.
[11] Q. Lin, X. Zhang, T. Wang, C. Zheng, X. Gao, Technical perspective of carbon capture, utilization, and storage, Engineering 14 (2022) 27–32, https://doi.org/10.1016/j.eng.2021.12.013.
[12] M. Mariyaselvakumar, G.G. Kadam, M. Mani, K. Srinivasan, L.J. Konwar, Direct hydrogenation of CO2-rich scrubbing solvents to formate/formic acid over heterogeneous Ru catalysts: a sustainable approach towards continuous integrated CCU, J. CO2 Util. 67 (2023), https://doi.org/10.1016/j.jcou.2022.102326.
[13] S. Nagireddi, J.R. Agarwal, D. Vedapuri, Carbon Dioxide Capture, Utilization, and Sequestration: Current Status, Challenges, and Future Prospects for Global Decarbonization, ACS Eng. Au 4 (1) (2023) 22–48, https://doi.org/10.1021/acsengineeringau.3c00049.
[14] H.O. LeClerc, H.C. Erythropel, A. Backhaus, D.S. Lee, D.R. Judd, M.M. Paulsen, M. Ishii, A. Long, L. Ratjen, G. Gonsalves Bertho, C. Deetman, Y. Du, M.K.M. Lane, P.V. Petrovic, A.T. Champlin, A. Bordet, N. Kaeffer, G. Kemper, J.B. Zimmerman, W. Leitner, P.T. Anastas, The CO2 tree: the potential for carbon dioxide utilization pathways, ACS Sustain. Chem. Eng. 13 (1) (2024) 5–29, https://doi.org/10.1021/acssuschemeng.4c07582.
[15] W. Wang, S. Wang, X. Ma, J. Gong, Recent advances in catalytic hydrogenation of carbon dioxide, Chem. Soc. Rev. 40 (7) (2011) 3703–3727, https://doi.org/10.1039/c1cs15008a.
[16] A. Alvarez, A. Bansode, A. Urakawa, A.V. Bavykina, T.A. Wezendonk, M. Makkee, J. Gascon, F. Kapteijn, Challenges in the greener production of formates/formic acid, methanol, and DME by heterogeneously catalyzed CO(2) hydrogenation processes, Chem. Rev. 117 (14) (2017) 9804–9838, https://doi.org/10.1021/acs.chemrev.6b00816.
[17] Z. Wang, Y. Kang, J. Hu, Q. Ji, Z. Lu, G. Xu, Y. Qi, M. Zhang, W. Zhang, R. Huang, L. Yu, Z.Q. Tian, D. Deng, Boosting CO(2) hydrogenation to formate over edge-sulfur vacancies of molybdenum disulfide, Angew. Chem. Int Ed. Engl. 62 (45) (2023) e202307086, https://doi.org/10.1002/anie.202307086.
[18] C. Wu, D. Wang, J. Guo, A. Zavabeti, P. Xiao, G.K. Li, Hollow hierarchical Pd/HNC nanoreactor as a high-performance catalyst for CO2 hydrogenation to formate, Energy Fuels 38 (4) (2024) 3357–3368, https://doi.org/10.1021/acs.energyfuels.3c05193.
[19] R. Chauvy, G. De Weireld, CO2 utilization technologies in Europe: a short review, Energy Technol. 8 (12) (2020), https://doi.org/10.1002/ente.202000627.
[20] W.Y. Hong, A techno-economic review on carbon capture, utilisation and storage systems for achieving a net-zero CO2 emissions future, Carbon Capture Sci. Technol. 3 (2022), https://doi.org/10.1016/j.ccst.2022.100044.
[21] C. Kim, K. Park, H. Lee, J. Im, D. Ususky, K. Tak, D. Park, W. Chung, D. Han, J. Yoon, H. Lee, H. Kim, Margareth, J. Jung, D.H. Won, C.-J. Yoo, K.B. Lee, K.-D. Jung, U. Lee, Accelerating the net-zero economy with CO2-hydrogenated formic acid production: process development and pilot plant demonstration, Joule 8 (3) (2024) 693–713, https://doi.org/10.1016/j.joule.2024.01.003.
[22] K. Park, G.H. Gunasekar, S.-H. Kim, H. Park, S. Kim, K. Park, K.-D. Jung, S. Yoon, CO2 hydrogenation to formic acid over heterogenized ruthenium catalysts using a fixed bed reactor with separation units, Green. Chem. 22 (5) (2020) 1639–1649, https://doi.org/10.1039/c9gc03685g.
[23] S. Ahn, K. Park, K.R. Lee, A. Haider, C.V. Nguyen, H. Jin, S.J. Yoo, S. Yoon, K.-D. Jung, Atomically dispersed Ru(III) on N-doped mesoporous carbon hollow spheres as catalysts for CO2 hydrogenation to formate, Chem. Eng. J. 442 (2022), https://doi.org/10.1016/j.cej.2022.136185.
[24] K.R. Lee, A. Haider, K. Park, S. Ahn, K.-D. Jung, Sustainable synthesis of N-doped carbon to stabilize Ru species for CO2 hydrogenation to formic acid, J. CO2 Util. 86 (2024), https://doi.org/10.1016/j.jcou.2024.102896.
[25] K.R. Lee, A. Masudi, K. Park, S. Ahn, J.S. Lee, S.J. Sim, K.-D. Jung, Sustainable approach for CO2 hydrogenation to formic acid with Ru single atom catalysts on nitrogen-doped carbon prepared from green algae, Chem. Eng. J. 494 (2024), https://doi.org/10.1016/j.cej.2024.152922.
[26] C. Li, G. He, Z. Qu, K. Zhang, L. Guo, T. Zhang, J. Zhang, Q. Sun, D. Mei, J. Yu, Highly dispersed Pd-CeO(x) nanoparticles in zeolite nanosheets for efficient CO(2)-mediated hydrogen storage and release, Angew. Chem. Int Ed. Engl. 63 (40) (2024) e202409001, https://doi.org/10.1002/anie.202409001.
[27] K. Park, K.R. Lee, S. Ahn, C.V. Nguyen, K.-D. Jung, Effects of the chemical states of N sites and mesoporosity of N-doped carbon supports on single-atom Ru catalysts during CO2-to-formate conversion, Appl. Catal. B Environ. Energy 346 (2024), https://doi.org/10.1016/j.apcatb.2024.123751.
[28] H. Park, K. Park, U. Lee, S. Yoon, Sustainable formate production via highly active CO(2) hydrogenation using porous organometallic polymer with ru-pnp active sites, ChemSusChem 18 (5) (2025) e202402038, https://doi.org/10.1002/cssc.202402038.
[29] A. Ajanovic, M. Sayer, R. Haas, The economics and the environmental benignity of different colors of hydrogen, Int. J. Hydrog. Energy 47 (57) (2022) 24136–24154, https://doi.org/10.1016/j.ijhydene.2022.02.094.
[30] H. Yoon, T. Yoon, H.-J. Yoon, C.-J. Lee, S. Yoon, Eco-friendly and techno-economic conversion of CO2into calcium formate, a valuable resource, Green. Chem. 24 (4) (2022) 1738–1745, https://doi.org/10.1039/d1gc04606c.
[31] J.M.M. Arcos, D.M.F. Santos, The hydrogen color spectrum: techno-economic analysis of the available technologies for hydrogen production, Gases 3 (1) (2023) 25–46, https://doi.org/10.3390/gases3010002.
[32] H. Yoon, T. Yoon, C.-J. Lee, S. Yoon, Kinetic conversion of magnesium and calcium ions of dolomite into useful value-added products using CO2, Chem. Eng. J. 469 (2023), https://doi.org/10.1016/j.cej.2023.143684.
[33] N. Athia, M. Pandey, M. Sen, S. Saxena, Factors affecting the economy of green hydrogen production pathways for sustainable development and their challenges, Environ. Sci. Pollut. Res. Int. 31 (32) (2024) 44542–44574, https://doi.org/10.1007/s11356-024-34096-x.
[34] E. Baraj, K. Ciahotný, T. Hlinčík, Advanced catalysts for the water gas shift reaction, Crystals 12 (4) (2022), https://doi.org/10.3390/cryst12040509.
[35] D.-H. Hwang, Y.-S. Choi, T.-W. Lim, Performance analysis in water-gas shift reactor for hydrogen yield improvement, J. Adv. Mar. Eng. Technol. 47 (4) (2023) 168–174, https://doi.org/10.5916/jamet.2023.47.4.168.
[36] V. Shilov, D. Potemkin, V. Rogozhnikov, P. Snytnikov, Recent advances in structured catalytic materials development for conversion of liquid hydrocarbons into synthesis gas for fuel cell power generators, Materials (Basel) 16 (2) (2023), https://doi.org/10.3390/ma16020599.
[37] L.L. Zhou, S.Q. Li, C. Ma, X.P. Fu, Y.S. Xu, W.W. Wang, H. Dong, C.J. Jia, F. R. Wang, C.H. Yan, Promoting molecular exchange on rare-earth oxycarbonate surfaces to catalyze the water-gas shift reaction, J. Am. Chem. Soc. 145 (4) (2023) 2252–2263, https://doi.org/10.1021/jacs.2c10326.
[38] J. Shabaker, Aqueous-phase reforming of methanol and ethylene glycol over alumina-supported platinum catalysts, J. Catal. 215 (2) (2003) 344–352, https://doi.org/10.1016/s0021-9517(03)00032-0.
[39] D. Preti, C. Resta, S. Squarcialupi, G. Fachinetti, Carbon dioxide hydrogenation to formic acid by using a heterogeneous gold catalyst, Angew. Chem. Int Ed. Engl. 50 (52) (2011) 12551–12554, https://doi.org/10.1002/anie.201105481.
[40] K.M. Yu, W. Tong, A. West, K. Cheung, T. Li, G. Smith, Y. Guo, S.C. Tsang, Non-syngas direct steam reforming of methanol to hydrogen and carbon dioxide at low temperature, Nat. Commun. 3 (2012) 1230, https://doi.org/10.1038/ncomms2242.

[41] E. Alberico, P. Sponholz, C. Cordes, M. Nielsen, H.J. Drexler, W. Baumann, H. Junge, M. Beller, Selective hydrogen production from methanol with a defined iron pincer catalyst under mild conditions, Angew. Chem. Int Ed. Engl. 52 (52) (2013) 14162–14166, https://doi.org/10.1002/anie.201307224.
[42] M. Nielsen, E. Alberico, W. Baumann, H.J. Drexler, H. Junge, S. Gladiali, M. Beller, Low-temperature aqueous-phase methanol dehydrogenation to hydrogen and carbon dioxide, Nature 495 (7439) (2013) 85–89, https://doi.org/10.1038/nature11891.
[43] R.E. Rodriguez-Lugo, M. Trincado, M. Vogt, F. Tewes, G. Santiso-Quinones, H. Grutzmacher, A homogeneous transition metal complex for clean hydrogen production from methanol-water mixtures, Nat. Chem. 5 (4) (2013) 342–347, https://doi.org/10.1038/nchem.1595.
[44] M.S. Jeletic, M.L. Helm, E.B. Hulley, M.T. Mock, A.M. Appel, J.C. Linehan, A cobalt hydride catalyst for the hydrogenation of CO2: pathways for catalysis and deactivation, ACS Catal. 4 (10) (2014) 3755–3762, https://doi.org/10.1021/cs5009927.
[45] A. Monney, E. Barsch, P. Sponholz, H. Junge, R. Ludwig, M. Beller, Base-free hydrogen generation from methanol using a bi-catalytic system, Chem. Commun. (Camb. 50 (6) (2014) 707–709, https://doi.org/10.1039/c3cc47306f.
[46] X. Min, M.W. Kanan, Pd-catalyzed electrohydrogenation of carbon dioxide to formate: high mass activity at low overpotential and identification of the deactivation pathway, J. Am. Chem. Soc. 137 (14) (2015) 4701–4708, https://doi.org/10.1021/ja511890h.
[47] J. Su, L. Yang, M. Lu, H. Lin, Highly efficient hydrogen storage system based on ammonium bicarbonate/formate redox equilibrium over palladium nanocatalysts, ChemSusChem 8 (5) (2015) 813–816, https://doi.org/10.1002/cssc.201403251.
[48] E. Alberico, A.J. Lennox, L.K. Vogt, H. Jiao, W. Baumann, H.J. Drexler, M. Nielsen, A. Spannenberg, M.P. Checinski, H. Junge, M. Beller, Unravelling the mechanism of basic aqueous methanol dehydrogenation catalyzed by Ru-PNP pincer complexes, J. Am. Chem. Soc. 138 (45) (2016) 14890–14904, https://doi.org/10.1021/jacs.6b05692.
[49] A. Kann, H. Hartmann, A. Besmehn, P.J.C. Hausoul, R. Palkovits, Hydrogenation of CO(2) to Formate over Ruthenium Immobilized on Solid Molecular Phosphines, ChemSusChem 11 (11) (2018) 1857–1865, https://doi.org/10.1002/cssc.201800413.
[50] S. Masuda, K. Mori, Y. Futamura, H. Yamashita, PdAg nanoparticles supported on functionalized mesoporous carbon: promotional effect of surface amine groups in reversible hydrogen delivery/storage mediated by formic acid/CO2, ACS Catal. 8 (3) (2018) 2277–2285, https://doi.org/10.1021/acscatal.7b04099.
[51] K. Mori, T. Sano, H. Kobayashi, H. Yamashita, Surface Engineering of a Supported PdAg Catalyst for Hydrogenation of CO(2) to Formic Acid: Elucidating the Active Pd Atoms in Alloy Nanoparticles, J. Am. Chem. Soc. 140 (28) (2018) 8902–8909, https://doi.org/10.1021/jacs.8b04852.
[52] J. Ye, R.C. Cammarota, J. Xie, M.V. Vollmer, D.G. Truhlar, C.J. Cramer, C.C. Lu, L. Gagliardi, Rationalizing the reactivity of bimetallic molecular catalysts for CO2 hydrogenation, ACS Catal. 8 (6) (2018) 4955–4968, https://doi.org/10.1021/acscatal.8b00803.
[53] H. Zhong, M. Iguchi, M. Chatterjee, T. Ishizaka, M. Kitta, Q. Xu, H. Kawanami, Interconversion between CO2 and HCOOH under Basic Conditions Catalyzed by PdAu Nanoparticles Supported by Amine-Functionalized Reduced Graphene Oxide as a Dual Catalyst, ACS Catal. 8 (6) (2018) 5355–5362, https://doi.org/10.1021/acscatal.8b00294.
[54] S. Kar, R. Sen, J. Kothandaraman, A. Goeppert, R. Chowdhury, S.B. Munoz, R. Haiges, G.K.S. Prakash, Mechanistic insights into ruthenium-pincer-catalyzed amine-assisted homogeneous hydrogenation of CO(2) to methanol, J. Am. Chem. Soc. 141 (7) (2019) 3160–3170, https://doi.org/10.1021/jacs.8b12763.
[55] Y. Pan, C. Guan, H. Li, P. Chakraborty, C. Zhou, K.W. Huang, CO(2) hydrogenation by phosphorus-nitrogen PN(3)P-pincer iridium hydride complexes: elucidation of the deactivation pathway, Dalton Trans. 48 (34) (2019) 12812–12816, https://doi.org/10.1039/c9dt01319a.
[56] R. Sun, A. Kann, H. Hartmann, A. Besmehn, P.J.C. Hausoul, R. Palkovits, Direct Synthesis of Methyl Formate from CO(2) With Phosphine-Based Polymer-Bound Ru Catalysts, ChemSusChem 12 (14) (2019) 3278–3285, https://doi.org/10.1002/cssc.201900808.
[57] K.J. Betsy, A. Lazar, A. Pavithran, C.P. Vinod, CO2 hydrogenation to formate by palladium nanoparticles supported on N-incorporated periodic mesoporous organosilica, ACS Sustain. Chem. Eng. 8 (39) (2020) 14765–14774, https://doi.org/10.1021/acssuschemeng.0c03860.
[58] S. Bhandari, S. Rangarajan, C.T. Maravelias, J.A. Dumesic, M. Mavrikakis, Reaction mechanism of vapor-phase formic acid decomposition over platinum catalysts: DFT, reaction kinetics experiments, and microkinetic modeling, ACS Catal. 10 (7) (2020) 4112–4126, https://doi.org/10.1021/acscatal.9b05424.
[59] Q. Sun, B.W.J. Chen, N. Wang, Q. He, A. Chang, C.M. Yang, H. Asakura, T. Tanaka, M.J. Hulsey, C.H. Wang, J. Yu, N. Yan, Zeolite-encaged Pd-Mn nanocatalysts for CO (2) hydrogenation and formic acid dehydrogenation, Angew. Chem. Int. Ed. Engl. 59 (45) (2020) 20183–20191, https://doi.org/10.1002/anie.202008962.
[60] H. Park, K. Park, K.-D. Jung, S. Yoon, CO2 hydrogenation into formate and methyl formate using Ru molecular catalysts supported on NNN pincer porous organic polymers, Inorg. Chem. Front. 8 (7) (2021) 1727–1735, https://doi.org/10.1039/d0qi01123a.
[61] G. Yang, Y. Kuwahara, K. Mori, C. Louis, H. Yamashita, PdAg alloy nanoparticles encapsulated in N-doped microporous hollow carbon spheres for hydrogenation of CO2 to formate, Appl. Catal. B Environ. 283 (2021), https://doi.org/10.1016/j.apcatb.2020.119628.
[62] Z. Zhang, S. Liu, M. Hou, G. Yang, B. Han, Continuous-flow formic acid production from the hydrogenation of CO2 without any base, Green. Chem. 23 (5) (2021) 1978–1982, https://doi.org/10.1039/d0gc04233a.
[63] S. Jiang, J. Yang, S. Zhai, L. Zhang, R. Tu, T. Yu, D. Zhai, L. Sun, W. Deng, G. Ren, Ambient hydrogen storage and release using CO2 and an l-Arginine-Functionalized PdAu catalyst via pH control, ACS Catal. 12 (22) (2022) 14113–14122, https://doi.org/10.1021/acscatal.2c03893.
[64] X. Xiao, J. Gao, S. Xi, S.H. Lim, A.K.W. Png, A. Borgna, W. Chu, Y. Liu, Experimental and in situ DRIFTs studies on confined metallic copper stabilized Pd species for enhanced CO2 reduction to formate, Appl. Catal. B Environ. 309 (2022), https://doi.org/10.1016/j.apcatb.2022.121239.
[65] L. Liu, A. Corma, Bimetallic sites for catalysis: from binuclear metal sites to bimetallic nanoclusters and nanoparticles, Chem. Rev. 123 (8) (2023) 4855–4933, https://doi.org/10.1021/acs.chemrev.2c00733.
[66] K. Mori, H. Hata, H. Yamashita, Interplay of Pd ensemble sites induced by GaO modification in boosting CO2 hydrogenation to formic acid, Appl. Catal. B Environ. 320 (2023), https://doi.org/10.1016/j.apcatb.2022.122022.
[67] Z. Wang, D. Ren, Y. He, M. Hong, Y. Bai, A. Jia, X. Liu, C. Tang, P. Gong, X. Liu, W. Huang, Z. Zhang, Tailoring electronic properties and atom utilizations of the pd species supported on anatase TiO2{101} for efficient CO2 hydrogenation to formic acid, ACS Catal. 13 (15) (2023) 10056–10064, https://doi.org/10.1021/acscatal.3c02428.
[68] C. Wu, M. Luo, Y. Zhao, S. Wang, X. Ma, A. Zavabeti, P. Xiao, G.K. Li, CO2 hydrogenation using MOFs encapsulated PdAg nano-catalysts for formate production, Chem. Eng. J. 475 (2023), https://doi.org/10.1016/j.cej.2023.146411.
[69] Y. Zhang, N. Levin, L. Kang, F. Muller, M. Zobel, S. DeBeer, W. Leitner, A. Bordet, Design and Understanding of Adaptive Hydrogenation Catalysts Triggered by the H (2)/CO(2)-Formic Acid Equilibrium, J. Am. Chem. Soc. 146 (44) (2024) 30057–30067, https://doi.org/10.1021/jacs.4c06765.
[70] G. Xue, Y. Jiao, X. Li, T. Lin, C. Yang, S. Chen, Z. Chen, H. Qi, S. Bartling, H. Jiao, H. Junge, M. Beller, CO-tolerant heterogeneous ruthenium catalysts for efficient formic acid dehydrogenation, Angew. Chem. Int Ed. Engl. 64 (4) (2025) e202416530, https://doi.org/10.1002/anie.202416530.
[71] W.L. Nelson, C.J. Engelder, The thermal decomposition of formic acid, J. Phys. Chem. 30 (4) (2002) 470–475, https://doi.org/10.1021/j150262a003.
[72] P. Poldorn, Y. Wongnongwa, T. Mudchimo, S. Jungsuttiwong, Theoretical insights into catalytic CO2 hydrogenation over single-atom (Fe or Ni) incorporated nitrogen-doped graphene, J. CO2 Util. 48 (2021), https://doi.org/10.1016/j.jcou.2021.101532.
[73] J. Kaishyop, T.S. Khan, S. Panda, P.R. Chandewar, D. Shee, T.C.R. Rocha, F. C. Vicentin, A. Bordoloi, Ni–N synergy enhanced the synthesis of formic acid via CO2 hydrogenation under mild conditions, Green. Chem. 25 (19) (2023) 7729–7742, https://doi.org/10.1039/d3gc01873c.
[74] D. Wei, H. Junge, M. Beller, An amino acid based system for CO(2) capture and catalytic utilization to produce formates, Chem. Sci. 12 (17) (2021) 6020–6024, https://doi.org/10.1039/d1sc00467k.
[75] S. Kushwaha, J. Parthiban, S.K. Singh, Recent developments in reversible CO(2) hydrogenation and formic acid dehydrogenation over molecular catalysts, ACS Omega 8 (42) (2023) 38773–38793, https://doi.org/10.1021/acsomega.3c05286.
[76] B. Loges, A. Boddien, F. Gärtner, H. Junge, M. Beller, Catalytic generation of hydrogen from formic acid and its derivatives: useful hydrogen storage materials, Top. Catal. 53 (13-14) (2010) 902–914, https://doi.org/10.1007/s11244-010-9522-8.
[77] K. Sordakis, C. Tang, L.K. Vogt, H. Junge, P.J. Dyson, M. Beller, G. Laurenczy, Homogeneous catalysis for sustainable hydrogen storage in formic acid and alcohols, Chem. Rev. 118 (2) (2018) 372–433, https://doi.org/10.1021/acs.chemrev.7b00182.
[78] C.H. Chen, S.L. Suib, Control of catalytic activity via porosity, chemical composition, and morphology of nanostructured porous manganese oxide materials, J. Chin. Chem. Soc. 59 (4) (2012) 465–472, https://doi.org/10.1002/jccs.201100699.
[79] M. Xu, Y. Sui, C. Wang, B. Zhou, Y. Wei, B. Zou, Design of porous Ag platelet structures with tunable porosity and high catalytic activity, J. Mater. Chem. A 3 (44) (2015) 22339–22346, https://doi.org/10.1039/c5ta07027a.
[80] M. Sabharwal, M. Secanell, Understanding the effect of porosity and pore size distribution on low loading catalyst layers, Electrochim. Acta 419 (2022), https://doi.org/10.1016/j.electacta.2022.140410.
[81] R.M. Mironenko, D.B. Eremin, V.P. Ananikov, The phenomenon of "dead" metal in heterogeneous catalysis: opportunities for increasing the efficiency of carbon-supported metal catalysts, Chem. Sci. 14 (48) (2023) 14062–14073, https://doi.org/10.1039/d3sc04691e.
[82] H. Park, S. Yoon, CO-Free H2 production by aqueous-phase reforming of methanol utilizing heterogenized Ru-MACHO at low temperature, ACS Sustain. Chem. Eng. 11 (32) (2023) 12036–12044, https://doi.org/10.1021/acssuschemeng.3c02330.
[83] S. Wild, C. Mahr, A. Rosenauer, T. Risse, S. Vasenkov, M. Baumer, New perspectives for evaluating the mass transport in porous catalysts and unfolding macro- and microkinetics, Catal. Lett. 153 (11) (2023) 3405–3422, https://doi.org/10.1007/s10562-022-04218-6.
[84] S. Padmanaban, G.H. Gunasekar, S. Yoon, Direct heterogenization of the ru-macho catalyst for the chemoselective hydrogenation of alpha,beta-unsaturated carbonyl compounds, Inorg. Chem. 60 (10) (2021) 6881–6888, https://doi.org/10.1021/acs.inorgchem.0c03681.
[85] M. Kass, A. Friedrich, M. Drees, S. Schneider, Ruthenium complexes with cooperative PNP ligands: bifunctional catalysts for the dehydrogenation of

ammonia-borane, Angew. Chem. Int Ed. Engl. 48 (5) (2009) 905–907, https://doi.org/10.1002/anie.200805108.
[86] J.B. Curley, C. Hert, W.H. Bernskoetter, N. Hazari, B.Q. Mercado, Control of Catalyst Isomers Using an N-Phenyl-Substituted RN(CH(2)CH(2)P(i)Pr(2))(2) Pincer Ligand in CO(2) Hydrogenation and Formic Acid Dehydrogenation, Inorg. Chem. 61 (1) (2022) 643–656, https://doi.org/10.1021/acs.inorgchem.1c03372.
[87] S. Kongkaew, M. Puripat, T. Kuamit, W. Parasuk, V. Parasuk, Importance of amine in carbon dioxide conversion to methanol catalyzed by Ru-PNP complex, Mol. Catal. 532 (2022), https://doi.org/10.1016/j.mcat.2022.112729.
[88] A. Moazezbarabadi, D. Wei, H. Junge, M. Beller, Improved CO(2) capture and catalytic hydrogenation using amino acid based ionic liquids, ChemSusChem 15 (23) (2022) e202201502, https://doi.org/10.1002/cssc.202201502.
[89] X. Yang, Mechanistic insights into ruthenium-catalyzed production of H2 and CO2 from methanol and water: a DFT study, ACS Catal. 4 (4) (2014) 1129–1133, https://doi.org/10.1021/cs500061u.
[90] N.S. Kumar, A. Adhikary, Transition metal pincer catalysts for formic acid dehydrogenation: a mechanistic perspective, Front. Chem. 12 (2024) 1452408, https://doi.org/10.3389/fchem.2024.1452408.